UCLA
UCLA Previously Published Works

Title

Alveolar macrophage lipid burden correlates with clinical improvement in patients with pulmonary alveolar proteinosis.

Permalink

https://escholarship.org/uc/item/8t20g57w

Journal

Journal of Lipid Research, 65(2)

Authors

Lee, Elinor
Williams, Kevin
McCarthy, Cormac
et al.

Publication Date

2024-01-06

DOI

10.1016/j.jlr.2024.100496

Copyright Information

Peer reviewed

Alveolar macrophage lipid burden correlates with clinical improvement in patients with pulmonary alveolar proteinosis

Elinor Lee[1,2], Kevin J. Williams[3], Cormac McCarthy[4,5], James P. Bridges[6], Elizabeth F. Redente[7,8], Thomas Q. de Aguiar Vallim[2,3,9,10,11,12], Robert A. Barrington[13,14], Tisha Wang[1,2], and Elizabeth J. Tarling[2,9,10,11,12]*

[1]Division of Pulmonary, Critical Care, and Sleep Medicine, David Geffen School of Medicine at University of California Los Angeles (UCLA), Los Angeles, CA, USA; [2]Department of Medicine, David Geffen School of Medicine at University of California Los Angeles (UCLA), Los Angeles, CA, USA; [3]Department of Biological Chemistry, David Geffen School of Medicine at University of California Los Angeles (UCLA), Los Angeles, CA, USA; [4]Department of Respiratory Medicine, St. Vincent's University Hospital, Dublin, Ireland; [5]School of Medicine, University College Dublin, Dublin, Ireland; [6]Division of Pulmonary, Critical Care and Sleep Medicine, and [7]Department of Pediatrics, National Jewish Health, Denver, CO, USA; [8]Department of Medicine, University of Colorado School of Medicine Aurora, CO, USA; [9]Division of Cardiology, David Geffen School of Medicine at University of California Los Angeles (UCLA), Los Angeles, CA, USA; [10]Molecular Biology Institute, and [11]Johnsson Comprehensive Cancer Center (JCCC), University of California Los Angeles (UCLA), Los Angeles, CA, USA; [12]Basic Liver Research Center at University of California Los Angeles (UCLA), Los Angeles, CA, USA; [13]Department of Microbiology & Immunology, and [14]Center for Lung Biology, University of South Alabama, Mobile, AL, USA

Pulmonary alveolar proteinosis (PAP) is a life-threatening, rare lung syndrome for which there is no cure and no approved therapies. PAP is a disease of lipid accumulation characterized by alveolar macrophage foam cell formation. While much is known about the clinical presentation, there is a paucity of information regarding temporal changes in lipids throughout the course of disease. Our objectives were to define the detailed lipid composition of alveolar macrophages in PAP patients at the time of diagnosis and during treatment. We performed comprehensive mass spectrometry to profile the lipid signature of alveolar macrophages obtained from three independent mouse models of PAP and from PAP and non-PAP patients. Additionally, we quantified changes in macrophage-associated lipids during clinical treatment of PAP patients. We found remarkable variations in lipid composition in PAP patients, which were consistent with data from three independent mouse models. Detailed lipidomic analysis revealed that the overall alveolar macrophage lipid burden inversely correlated with clinical improvement and response to therapy in PAP patients. Specifically, as PAP patients experienced clinical improvement, there was a notable decrease in the total lipid content of alveolar macrophages. This crucial observation suggests that the levels of these macrophage-associated lipids can be utilized to assess the efficacy of treatment. ▓ These findings provide valuable insights into the dysregulated lipid metabolism associated with PAP, offering the potential for lipid profiling to serve as a means of monitoring therapeutic interventions in PAP patients.

Supplementary key words Cholesterol • foam cells • lipidomics • lipids • phospholipids • pulmonary surfactant • pulmonary alveolar proteinosis • alveolar macrophages

Pulmonary alveolar proteinosis (PAP) is a rare lung disorder with no cure or approved therapies (1). PAP is primarily a disease of surfactant and lipid accumulation within alveolar macrophages that arises due to various biochemical defects. It is categorized into primary, secondary, and congenital etiologies (2). The most common form of disease is primary PAP that occurs either from high levels of neutralizing antibodies to granulocyte macrophage colony stimulating factor (GM-CSF) or from hereditary mutations in the GM-CSF receptor (3, 4). Congenital PAP is the rarest disease type caused by mutations in genes that are essential for surfactant production (2). Secondary PAP is associated with underlying diseases that secondarily affect alveolar macrophages (1). Approximately 90% of patients have primary autoimmune PAP (aPAP), characterized by the presence of autoantibodies against GM-CSF, leading to the disruption of GM-CSF signaling in alveolar macrophages (1). GM-CSF is a key pulmonary hormone that mediates alveolar macrophage

---

*For correspondence: Elizabeth J. Tarling, etarling@mednet.ucla.edu.

maturation and self-renewal (5, 6). In the absence of GM-CSF signaling, alveolar macrophages are impaired in their ability to regenerate and mature and also catabolize surfactant (6). Mice deficient in GM-CSF ($Csf2^{-/-}$) or its receptor ($Csf2ra^{-/-}$ and $Csf2rb^{-/-}$) develop PAP-like pulmonary histopathology and are used as preclinical mouse models to study PAP (7–9). Current treatment is limited and focused on managing symptoms and treating disease complications. The standard of care is whole lung lavage (WLL), which is invasive, not widely available, and often only transiently effective; however, some experimental therapies including administration of inhaled GM-CSF have shown recent promise (2, 10).

We and others have demonstrated that alveolar macrophages isolated from either PAP patients or $Csf2^{-/-}$ and $Csf2rb^{-/-}$ mice have increased levels of cholesterol in addition to changes in the levels of triglycerides (TGs), free fatty acids (FFAs), and phospholipid species compared to macrophages obtained from healthy counterparts (11, 12). Alveolar macrophages isolated from PAP patients or mouse models of PAP have also been shown to have significantly lower expression of ATP-binding cassette transporter family member G1 (ABCG1) and peroxisome proliferator-activated receptor gamma, important mediators of cholesterol and lipid efflux from macrophages (13–18). We recently reported that treatment of a subset of PAP patients with statins, a class of drugs commonly used to treat hypercholesterolemia due to their ability to lower plasma cholesterol levels, markedly reduced pulmonary abnormalities and improved PAP disease (11). Further, we demonstrated that statin treatment reduced alveolar macrophage cholesterol content by increasing cholesterol efflux (11). Taken together, these data are consistent with the idea that alterations in lipid homeostasis, and particularly cholesterol homeostasis, have a significant role in the pathogenesis of PAP (11, 12).

Although the lipid composition of bronchoalveolar lavage fluid (BALF) from patients with PAP was recently described (19), the detailed lipidome of alveolar macrophages, the main cell type that drives pathogenesis of PAP, remains unknown. We reasoned that understanding the lipid composition of these key effector cells could provide new insights into the mechanisms underlying PAP, contribute to a better understanding of disease progression, and potentially identify novel therapeutic targets. We also hypothesized that because reducing macrophage cholesterol content is associated with improved disease (11), changes in lipid composition may correlate with a patient's clinical course and disease progression, an area that represents a significant unmet need in the PAP patient community.

To address these knowledge gaps, we utilized unbiased comprehensive mass spectrometry to profile and quantify the lipidome of alveolar macrophages from non-PAP and PAP patients. In addition, the lipid profile of alveolar macrophages from PAP patients during their clinical course was also examined. We found remarkable variations in lipid composition both among individual PAP patients and compared to non-PAP patients, consistent with data obtained from animal models of PAP. We also observed that the overall lipid burden in alveolar macrophages correlated with clinical improvement and the response to therapy in PAP patients. Specifically, as patients experienced clinical improvement, there was a significant decrease in the total lipid content of alveolar macrophages. These data represent a significant advancement in our understanding of human PAP disease and shed light on the role of macrophage-associated lipids in disease severity. The correlation between lipid composition and disease progression holds promise for developing biomarkers that can aid in monitoring disease progression and response to therapy.

MATERIALS AND METHODS

Patients and ethical approvals

All patients included in this study were male and female adults who have underlying non-PAP (n = 11) pulmonary disease or autoimmune PAP (n = 8) and are being treated at the University of California, Los Angeles. Ages ranged from 26 to 72 years old. The institutional review board of the University of California, Los Angeles, approved this study (IRB#0003456). All human participants provided written informed consent according to the Declaration of Helsinki.

Collection of human and mouse bronchoalveolar fluid

Human bronchoalveolar (BAL) fluid was collected from discarded material of non-PAP patients (n = 11) undergoing bronchoscopy with diagnostic BAL or PAP patients (n = 8) undergoing therapeutic WLL. Non-PAP patients had bronchoscopies with BAL performed to evaluate for non-PAP related issues, including infections and airway complications. None of these patients went on to develop secondary PAP. Mouse BAL fluid was collected from mice as previously described (14).

Mice

$Abcg1^{-/-}$ (16, 20), $Csf2rb^{-/-}$ (9), and $Rasgrp1^{-/-}$ (18), mice on a C57BL6/J background were generated as previously described. All animals were maintained on normal rodent diet (5001; Ralston Purina Company) at UCLA on a 12 h/12 h light/dark cycle with unlimited access to food and water. Animals used in this study ranged from 6–8 weeks ($Csf2rb^{-/-}$) to 8–12 months of age ($Abcg1^{-/-}$ and $Rasgrp1^{-/-}$). All animal experiments were approved by the Office of Animal Research Oversight and the Institutional Care and Use Committee at the University of Los Angeles.

Isolation of alveolar macrophages

Alveolar macrophages were isolated from human or mouse BAL by low-spin centrifugation to preserve cellular integrity at 200 g for 5 min. Cells were washed and resuspended with Ammonium-Chloride-Potassium lysing buffer to lyse red

blood cells. Cells were counted and aliquoted at 2×10^6 or 5×10^6 cells in 200 µl of phosphate-buffered solution (PBS) before being stored at −80°C. Macrophage purity was >95% as previously described (14, 17). For frozen samples, cells were frozen immediately at −80°C and counted after being thawed and prior to lipid extraction. The duration of the cells in the freezer ranged from 0.1 to 8 years before analysis. Long-term stability of the cells and lipids in human lavage fluid for these lengths of time has been previously described (19).

Lipid extraction and lipidomic analysis

A modified Bligh and Dyer extraction was performed on human alveolar macrophages (21, 22). For alveolar macrophages, 5×10^6 cells were resuspended in 200 µl of PBS. Prior to the biphasic extraction, the 54 internal standard Lipidyzer Mix (supplemental Table S1) was added to each sample to quantify 13 different subclasses (AB Sciex, 5040156). In later experiments (analyzed after 2021), a 74 standard mixture was utilized to measure 17 lipid subclasses (Avanti 330820, 861809, 330726, 330729, 330727, 791642). Following two successive extractions, pooled organic layers were dried down in a Genevac EZ-2 Elite. Lipid samples were resuspended in 1:1 methanol/dichloromethane with 10 mM ammonium acetate and transferred to robovials (Thermo, 10,800,107) for analysis.

Samples were analyzed by direct infusion on a Sciex 5500 with differential mobility device (comparable to Sciex Lipidyzer Platform) with a targeted acquisition list consisting of ~1100 lipid species (supplemental Table S2). Later experiments (analyzed after 2021) were analyzed using an expanded acquisition list targeting 1450 lipid species. The differential mobility device was tuned with SelexION tuning kit (Sciex, 5040141) or EquiSPLASH LIPIDOMIX (Avanti, 330731). Data analysis was performed with in-house data analysis workflow. Instrument settings, MRM lists, and analysis method are available for original and expanded methods (23). Quantitative values were normalized to cell counts. Fatty acids identified represent species composition but not positional specificity.

Processing and analysis of samples for gas chromatography/mass spectrometry

For alveolar macrophages, 2×10^6 cells were resuspended in 200 µl of PBS to perform acid methanolysis with methanol, toluene, and hydrochloric acid (HCl). Standards were created from a stock cholesterol standard (Avanti Polar Lipids, 700000P-100 mg) and diluted with hexane. Prior to adding the acid methanolysis mix, a stigmastanol internal standard lipid was added to each sample and standard. Once the mix was added, the samples were incubated at 45°C for about 8–12 h. Then, lipids were extracted by adding 1:1 0.4 M NaCl and hexane, mixing, spinning, and transferring the top layer to new tubes. This then underwent cholesterol derivatization via sialylation reaction with pyridine (Sigma, 270,970-100 ml) and N,O-Bis(trimethylsilyl)trifluoroacetamide with trimethylchlorosilane (Supelco, 33,155-4) before being run on the gas chromatography/mass spectrometry (GC-MS) machine to measure total cholesterol. The instrument settings and tuning settings are available upon request. The data were analyzed on the MassHunter software with quantitative values being normalized to cell counts.

Statistical analysis

Results are represented as mean ± SEM. Statistical analysis was performed using GraphPad Prism 8 software. We analyzed data for Gaussian distribution using the Shapiro–Wilk normality test. Data that were determined to be parametric were analyzed by unpaired two-tailed Student's t test to compare two independent groups or by paired two-tailed Student's t test to compare two time points. Data determined to be nonparametric were analyzed by Mann-Whitney U-test for comparison of two groups. N and P values are reported in the figure legends. P value <0.05 was used to indicate statistical significance.

RESULTS

Extensive lipid heterogeneity in animal models of PAP

PAP is primarily a disease of lipid and surfactant accumulation, yet the detailed lipidome of alveolar macrophages, the main cell type driving pathogenesis of PAP, remains unknown. To gain a better understanding of the lipid composition in PAP, we first sought to establish the detailed lipid profile in different mouse models of PAP. Lipids were extracted from whole lung tissue from wild type, $Csf2rb^{-/-}$ (a model of primary hereditary PAP), $Rasgrp1^{-/-}$ (a model of autoimmune PAP), and $Abcg1^{-/-}$ (a model of spontaneous PAP) mice and analyzed by mass spectrometry. As expected, all PAP mice had increased total lipid content in their lungs (**Fig. 1**A). Unbiased shotgun lipidomic profiling revealed significant increases in phosphatidylcholine (PC) (Fig. 1B; teal; supplemental Fig. S1A) and cholesterol ester (CE) (Fig. 1B; red; supplemental Fig. S1E) in the lungs of mice with PAP, consistent with previous reports by us and others (11, 12, 19). We also noted significant increases in phosphatidylethanolamine (PE) (Fig. 1B; orange) and sphingomyelin (SM) (Fig. 1B; salmon), along with significant decreases in TGs (Fig. 1B; yellow) and FFAs (Fig. 1B; green). We then stratified mice with PAP by the pathogenesis of disease. We observed striking differences in the lipid composition in the lungs of mice with PAP (Fig. 1C–E; supplemental Fig. S1B–D, F–H). $Abcg1^{-/-}$ mice, a model of spontaneous PAP, had marked increases in both CE and PC (Fig. 1C–E), accompanied by smaller increases in PE (Fig. 1C). In contrast, $Csf2rb^{-/-}$ mice, a model of hereditary PAP, primarily had increased PC (Fig. 1C, D), with modest increases in CE content (Fig. 1C, E), and decreased PE content (Fig. 1C, F). $Rasgrp1^{-/-}$, a recently described model of autoimmune PAP (18), demonstrated an intermediate phenotype with large increases in PC (Fig. 1C, D) and PE (Fig. 1C, F) and modestly increased CE (Fig. 1C, E).

Analysis of the individual PC species demonstrated that although the different models of PAP accrued PC to varying degrees (Fig. 1G and supplemental Fig. S1C, D), there were more similarities in the types of PC species that accumulate. Interestingly, the composition of PC species was remarkably similar among $Csf2rb^{-/-}$, $Rasgrp1^{-/-}$, and wild-type animals (Fig. 1G; pie chart), whereas $Abcg1^{-/-}$ mice accumulated proportionally
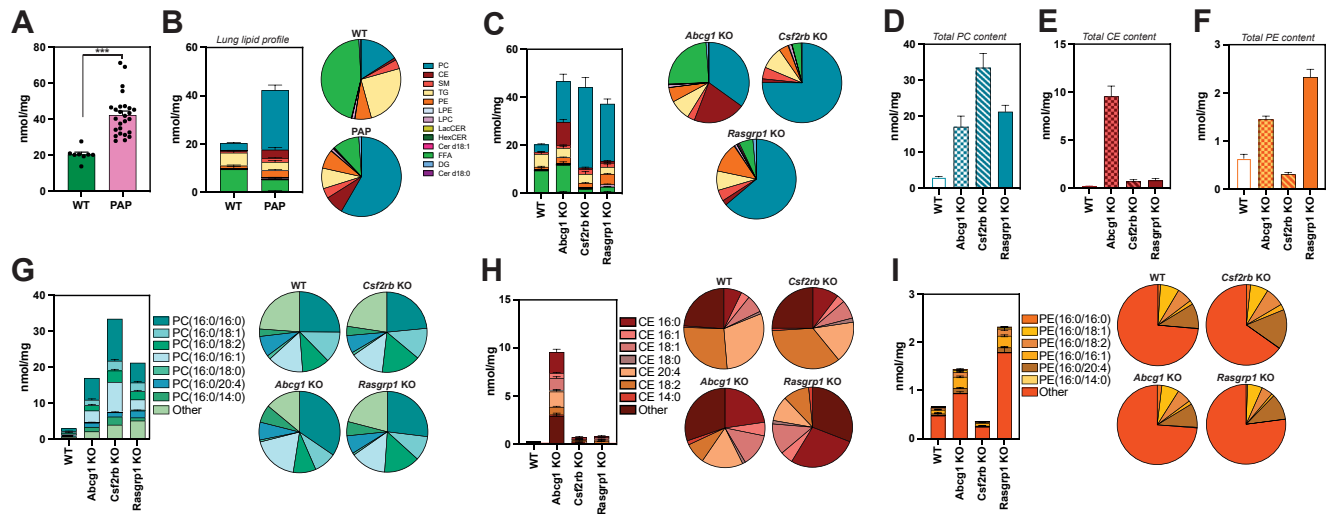
Fig. 1. In-depth lipidomic profiling reveals heterogeneity among animal models of PAP. A: Quantitative measurement of lipid class profile in alveolar macrophages from wild-type mice and mice with PAP. B: Compositional lipid analysis of alveolar macrophages from wild-type mice and mice with PAP. (C) Compositional lipid analysis of alveolar macrophages from wild type, $Abcg1^{-/-}$, $Csf2rb^{-/-}$, and $Rasgrp1^{-/-}$ mice. D–F: Total PC (D), CE (E), and PE (F) content in alveolar macrophages from wild type, $Abcg1^{-/-}$, $Csf2rb^{-/-}$, and $Rasgrp1^{-/-}$ mice. G–I: Composition analysis of PC (G), CE (H), and PE (I) species in alveolar macrophages from wild type, $Abcg1^{-/-}$, $Csf2rb^{-/-}$, and $Rasgrp1^{-/-}$ mice. All samples are run in triplicate. Data are mean ± SEM. Significance was determined at $P < 0.05$ by Student's t test (A), or Kruskal-Wallis test with Dunn's correction (D–F). ***$P < 0.001$.

more PC16:0/16:0 and PC16:0/16:1 (Fig. 1G; pie chart). There were striking differences in the amount of CE accumulation between the different animal models of PAP, with $Abcg1^{-/-}$ mice accumulating significantly more CE than either $Csf2rb^{-/-}$ or $Rasgrp1^{-/-}$ animals (Fig. 1H and supplemental Fig. S1G, H). There was further discordance in the types of CE species accumulating. The composition of CE species was similar between $Csf2rb^{-/-}$ and wild-type animals (Fig. 1H; pie chart). In contrast to PC species, the CE composition of $Rasgrp1^{-/-}$ animals was more similar to that of $Abcg1^{-/-}$ animals (Fig. 1H; pie chart). Despite the marked differences in the amount of PE accumulating (Fig. 1F, I), there were relatively minor differences in the composition of PE species among the different animal models of PAP pathogenesis (Fig. 1I; pie chart). Together, these data demonstrate that there are important differences in lipid homeostasis and composition in different animal models of PAP.

Alveolar macrophages from PAP patients show broad changes in lipid homeostasis

We next wanted to examine whether this heterogeneity in lipid composition existed in human patients with PAP. In order to define the lipid signature in PAP patients, we obtained alveolar macrophages from bronchoscopy with BAL on non-PAP (Table 1) and WLL on PAP patients (Table 2). Lipids were extracted from isolated macrophages and analyzed by mass spectrometry.

Consistent with our data from animal models of PAP (Fig. 1), alveolar macrophages from PAP patients demonstrated an overall increase in total lipid content compared to non-PAP patients (**Fig. 2**A). The predominant lipid class recovered in both non-PAP and PAP alveolar macrophages was PC (Fig. 2A, B; teal). Individual lipid profiles of non-PAP patients displayed broad heterogeneity in terms of lipid composition (Fig. 2C and supplemental Fig. S2A), possibly due to individual variability or the variety of pulmonary pathologies present in these patients (Table 1). Importantly, none of these patients went on to develop secondary or acquired PAP. In almost all of the non-PAP patients, the major lipids recovered from macrophages were PC and PE (Fig. 2B, C; teal and orange, respectively). These cells contained lower abundance of other major lipid classes, which included FFA (green), SM (salmon), TG (yellow), and CE (red) (Fig. 2B, C). Overall, we observed a marked difference in the lipid composition of the alveolar macrophages from PAP patients compared to non-PAP patients (Fig. 2B and supplemental Fig. S2A, B). In non-PAP alveolar macrophages, PC and PE species represent 46% and 18%, respectively, of the total lipid (Fig. 2B), whereas in PAP alveolar macrophages, PC represents almost 75% of the total lipid, and PE represents only 2% (Fig. 2B). We also performed lipidomic profiling on the clear (cell-free) BALF fluid (supplemental Fig. S2C). We observed that the total lipid content was increased 2-fold in BALF from PAP patients compared to non-PAP patients; however, there was no significant change in lipid composition.

In all PAP patient alveolar macrophage samples, the predominant lipid species recovered was PC (Fig. 2B, D), with levels increased 3-fold in PAP alveolar macrophages compared to non-PAP alveolar macrophages

TABLE 1. Characteristics of 11 non-PAP patients

Characteristics	Non-PAP 1	Non-PAP 2	Non-PAP 3	Non-PAP 4	Non-PAP 5	Non-PAP 6	Non-PAP 7	Non-PAP 8	Non-PAP 9	Non-PAP 10	Non-PAP 11
Age (years old)	71	72	60	49	63	65	59	35	68	63	48
Sex	Male	Male	Male	Male	Male	Male	Female	Female	Male	Female	Male
Race	White	Black	White	White	Asian	White	White	Asian	White	Hispanic	Black
BMI	18.5–24.9	25–29.9	25–29.9	25–29.9	25–29.9	25–29.9	18.5–24.9	25–29.9	25–29.9	25–29.9	30–39.9
Diagnosis	Lung nodules	Lung cancer	Bronchi-ectasis	Tracheal stenosis	Lung cancer	Met head and neck cancer	Familial ILD	CTD-ILD	COPD	RA-ILD	Sarcoidosis
Lung transplant status	No	No	No	No	No	No	Post	Post	Post	Post	Post
Smoking status	Former	Former	Never	Former	Former	Former	Never	Never	Former	Never	Never
Comorbidities											
Hyperlipidemia	Yes	Yes	No	No	No	Yes	No	No	Yes	Yes	Yes
Hypertension	Yes	No	No	No	No	Yes	Yes	No	Yes	No	Yes
Diabetes	No	No	No	No	No	No	No	No	Yes	No	No

(Fig. 2E). Absolute levels of CE were significantly higher (2-fold) in PAP alveolar macrophages (Fig. 2F). Consistent with our previously published data (11), total cholesterol content as measured by GC-MS was significantly elevated (7-fold) in PAP compared to non-PAP alveolar macrophages (Fig. 2G). Lysophosphatidylcholine (LPC; lilac) levels were elevated 11-fold in PAP alveolar macrophages compared to non-PAP alveolar macrophages, while lactosylceramides, PE, and TG were all significantly decreased by 13.8-fold, 5.3-fold, and 4.8-fold, respectively (Fig. 2H). We observed smaller increases in d18:1 sphingosine ceramides (Cer d18:1) and FFAs, with no significant differences in diacylglycerol, d18:0 ceramides, hexosyl ceramides, LPE, and SM (supplemental Fig. S2D).

When we specifically compared PAP patients with fibrosis (PAP6, PAP7, and PAP8) to PAP patients without fibrosis, we found that PAP patients with fibrosis have significantly increased lipid content within their alveolar macrophages (Fig. 2I). There are specific increases in CE (supplemental Fig. S2E) that are accompanied by increases in Cer d18:1, hexosyl ceramides, LPC, LPE, and TG (supplemental Fig. S2F). Taken together, these data suggest that, in addition to the previously observed increases in PC and cholesterol, these broad changes in lipid metabolism in alveolar macrophages from PAP patients may have important implications for disease pathogenesis and progression.

The major surfactant lipid recovered in both non-PAP and PAP macrophages is PC (Fig. 2A). However, we also identified significant differences in PC species composition in alveolar macrophages between PAP and non-PAP patients (Fig. 3A, B) (19, 24). In non-PAP alveolar macrophages, PC containing 16:0/16:0 or 16:0/18:1 fatty acids represent approximately 27% and 20% of the total cellular PC, respectively (Fig. 3B). In contrast, in PAP alveolar macrophages, PC16:0/16:0 represents almost 50% and PC16:0/18:1 represents only 13% of the total cellular PC (Fig. 3B). Furthermore, both the saturated (Fig. 3C) and unsaturated (Fig. 3D) PC content were significantly increased in PAP macrophages, compared to non-PAP macrophages. Similar to what we observed with PC species composition (Fig. 3B), the composition of CE species was significantly altered (Fig. 3F). The most abundant CE species in non-PAP alveolar macrophages was CE18:2, whereas in PAP alveolar macrophages, the predominant CE species were CE16:0 and CE18:0 (Fig. 3F). Saturated CE16:0 and unsaturated CE18:2 represent approximately 15% and 33% of the total CE, respectively, in non-PAP alveolar macrophages (Fig. 3F). In contrast, in PAP alveolar macrophages, CE16:0 and CE18:2 represent 30% and 20% of total CE species, respectively (Fig. 3F). These changes are reflected by a significant increase in total saturated CE content in PAP alveolar macrophages but no significant difference in unsaturated content (Fig. 3G, H). Following our observations that additional lipids are also altered in PAP alveolar macrophages

TABLE 2. Characteristics of eight autoimmune PAP patients

Characteristics	PAP 1	PAP 2	PAP 3	PAP 4	PAP 5	PAP 6	PAP 7	PAP 8
Age (years old)	42	54	50	63	29	59	34	26
Sex	Male	Female	Male	Female	Male	Male	Female	Female
Race	White	Black	Black	Hispanic	White	Asian	Hispanic	Black
BMI	18.5–24.9	>40	25–29.9	30–39.9	25–29.9	18.5–24.9	18.5–24.9	25–29.9
Imaging - presence of pulmonary fibrosis	No	No	No	No	No	Yes	Yes	Yes
Treatment (apart from WLL)	Inhaled GM-CSF	Statin	Rituximab, plasmapheresis, statin, pioglitazone	Statin	None	Statin	Inhaled GM-CSF, statin, pioglitazone, Rituximab, plasmapheresis	None
Smoking status	Never	Never	Never	Never	Never	Never	Never	Never
Comorbidities								
Hyperlipidemia	No	Yes	Yes	Yes	No	Yes	No	No
Hypertension	No	Yes	Yes	Yes	No	Yes	No	Yes
Diabetes	No	No	Yes	Yes	No	Yes	No	No

(Fig. 2I), we performed further compositional analysis (supplemental Fig. S3). There were striking changes in diacylglycerol, lactosylceramide, LPC, PE, and SM composition (supplemental Fig. S3). Together, these data demonstrate significant changes in alveolar macrophage lipid composition in addition to the well-documented accumulation of surfactant PC in patients with PAP.

Lipid profile of alveolar macrophages correlates with clinical improvement

PAP patients often display variable disease progression ranging from progressive deterioration to stable, yet unremitting disease, to clinical improvement. However, the reasons underlying these marked differences are not well understood. Further, there are no validated or reliable biomarkers of a patient's disease progression or response to therapy. Because PAP is a disease of lipid accumulation, we hypothesized that the lipid profile (composition and/or total lipid level) of alveolar macrophages would correlate with a patient's disease progression or regression. Here, we provide detailed analysis of PAP patients displaying different disease progression and the relative change in their alveolar macrophage lipid profiles.

The first patient, PAP 1, is an otherwise healthy 42-year-old male, who was diagnosed with aPAP in early 2014 (Fig. 4). He required 2–3 WLL per year due to
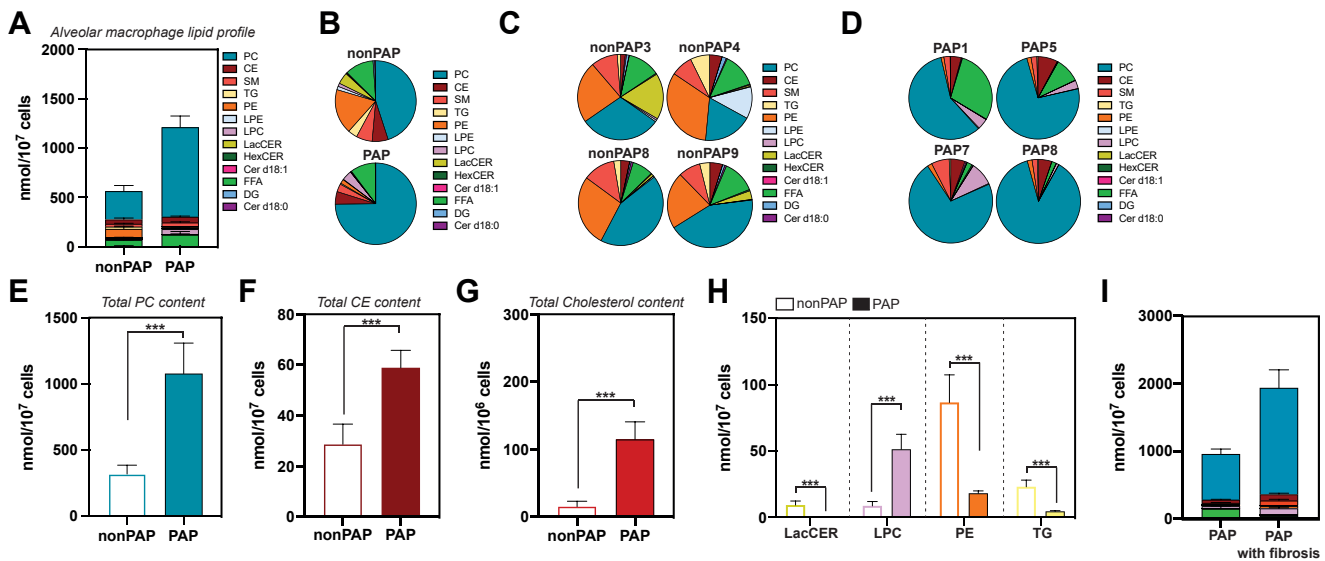

Fig. 2. High-resolution unbiased lipidomic profiling reveals broad changes in lipid metabolism in PAP alveolar macrophages. A: Quantitative measurement of lipid class profile in alveolar macrophages of non-PAP patients versus PAP patients. B: Compositional lipid analysis of alveolar macrophages from PAP patients compared to non-PAP patients. C, D: Quantitative compositional analysis of lipid classes in alveolar macrophages of individual non-PAP patients (C) and PAP patients (D). E, F: Total PC (E) and CE (F) content in non-PAP versus PAP patients. G: Total cholesterol content measured by GC/MS in alveolar macrophages of PAP patients compared to non-PAP patients. H: Total LacCer, LPC, PE, and TG content in alveolar macrophages of non-PAP and PAP patients. I: Quantitative measurement of lipid class profile in alveolar macrophages of PAP patients and PAP patients with fibrosis. All samples are run in duplicate or triplicate. Data are mean ± SEM. Significance was determined at $P < 0.05$ by Student's t test (E–H). ***$P < 0.001$.
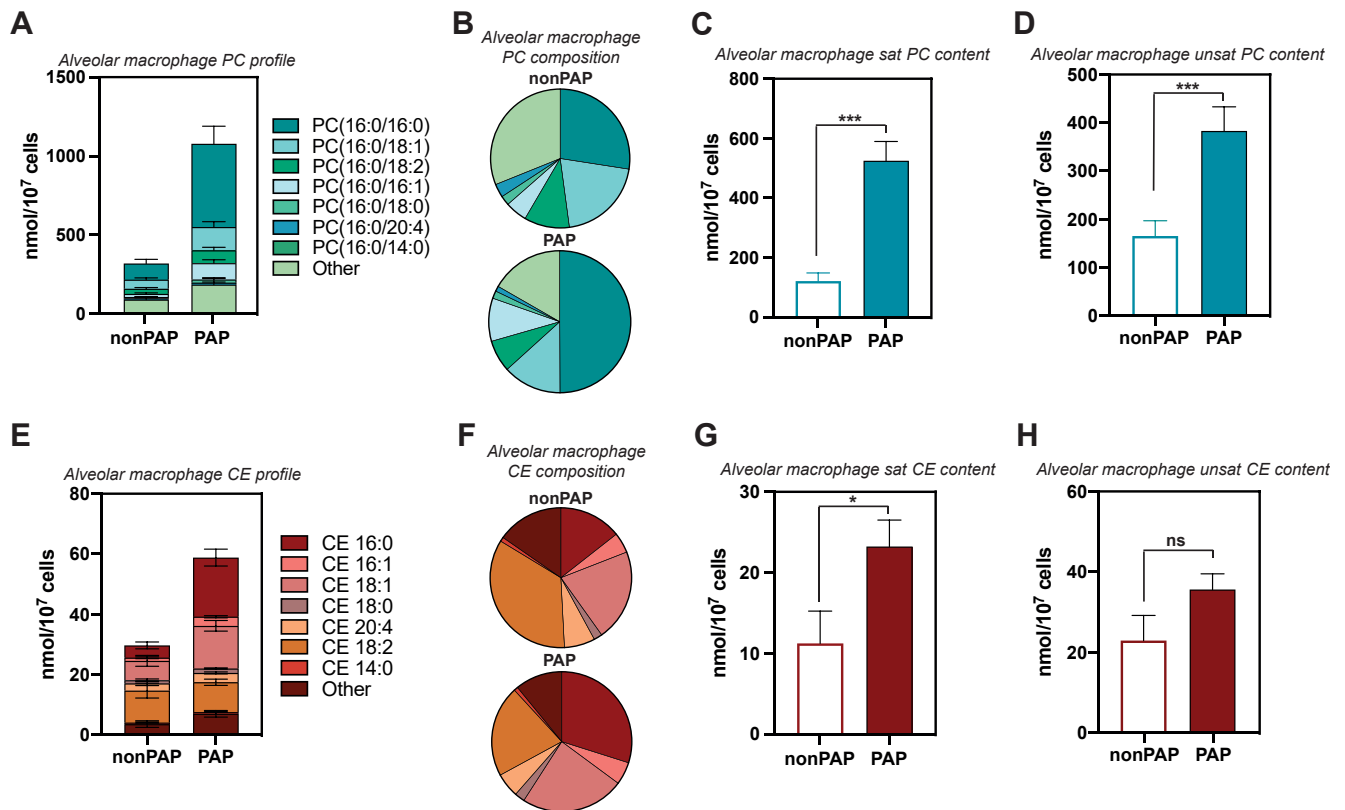
Fig. 3. PAP alveolar macrophages display a significant shift in lipid compositional content. A, B: Absolute quantification (A) and compositional analysis (B) of the most abundant PC species, including PC(16:0/16:0), PC(16:0/16:1), PC(16:0/18:0), PC(16:0/18:1), PC(16:0/18:2), and PC(16:0/20:4), in alveolar macrophages from PAP patients compared to non-PAP patients. C, D: Quantitative measurement of saturated (C) and unsaturated (D) PC content in alveolar macrophages from non-PAP versus PAP patients. (E, F) Absolute quantification (E) and compositional analysis (F) of the most abundant CE species, including CE(14:0), CE(16:0), CE(16:1), CE(18:0), CE(18:1), CE(18:2), and CE(20:4), in alveolar macrophages from PAP patients compared to non-PAP patients. G, H: Quantitative measurement of saturated (G) and unsaturated (H) CE content in alveolar macrophages from non-PAP versus PAP patients. All samples are run in duplicate or triplicate. Data are mean ± SEM. Significance was determined at $P < 0.05$ by Student's t test (C, D, G, H). $*P < 0.05$, $***P < 0.001$.

dyspnea before being initiated on inhaled GM-CSF in February 2016 (Fig. 4A). After receiving inhaled GM-CSF for approximately 9 months, his clinical status improved markedly, and he has not required further WLL to date (Fig. 4A). Clinical improvement is evidenced by decreased ground glass opacities (red asterisk) and septal thickening (red arrowhead) on imaging between his diagnostic CT in 2014 prior to treatment (Fig. 4B, No Tx) and his 2018 CT after receiving multiple WLL and inhaled GM-CSF (Fig. 4B, WLL+Tx).

Alveolar macrophages were obtained in 2014 shortly after diagnosis and after initiation on inhaled GM-CSF (Fig. 4A; blue boxes). Unbiased lipidomic profiling revealed that the most abundant lipid classes were PC, FFAs, and CE. Consistent with his noted clinical improvement (Fig. 4B, WLL+Tx), the total lipid content and overall levels of all major lipid classes decreased after 10 months of inhaled GM-CSF therapy (Fig. 4C, D). These data demonstrate that the macrophages present in the alveolar space after 10 months of GM-CSF have lipid profiles that are more similar to those seen in non-PAP cells, consistent with normal, or near-normal,

macrophage lipid metabolism. Total cholesterol levels as measured by GC-MS were also significantly decreased after being on inhaled GM-CSF, indicating improvement in surfactant lipid catabolism (Fig. 4E). The overall amount of PC and CE species significantly decreased after the patient was placed on inhaled GM-CSF (Fig. 4F, G). Surprisingly, PC and CE species compositions were not drastically altered in alveolar macrophages before and after GM-CSF inhalation (Fig. 4F, G), suggesting that changes in overall macrophage lipid burden are more reflective of clinical improvement. We observed similar findings in a second patient, PAP 3 (supplemental Fig. S4). He is a 50-year-old male diagnosed with aPAP in 2010, who was taking oral statin therapy for hyperlipidemia. He received subcutaneous injections of GM-CSF, multiple doses of rituximab, and repeated rounds of plasmapheresis, before being placed on pioglitazone and inhaled GM-CSF in addition to his continued oral statin (supplemental Fig. S4A). Since 2021, he has not required further WLL (supplemental Fig. S4A), indicating some degree of clinical improvement. Alveolar macrophages were obtained in 2019 before initiation of inhaled GM-CSF and
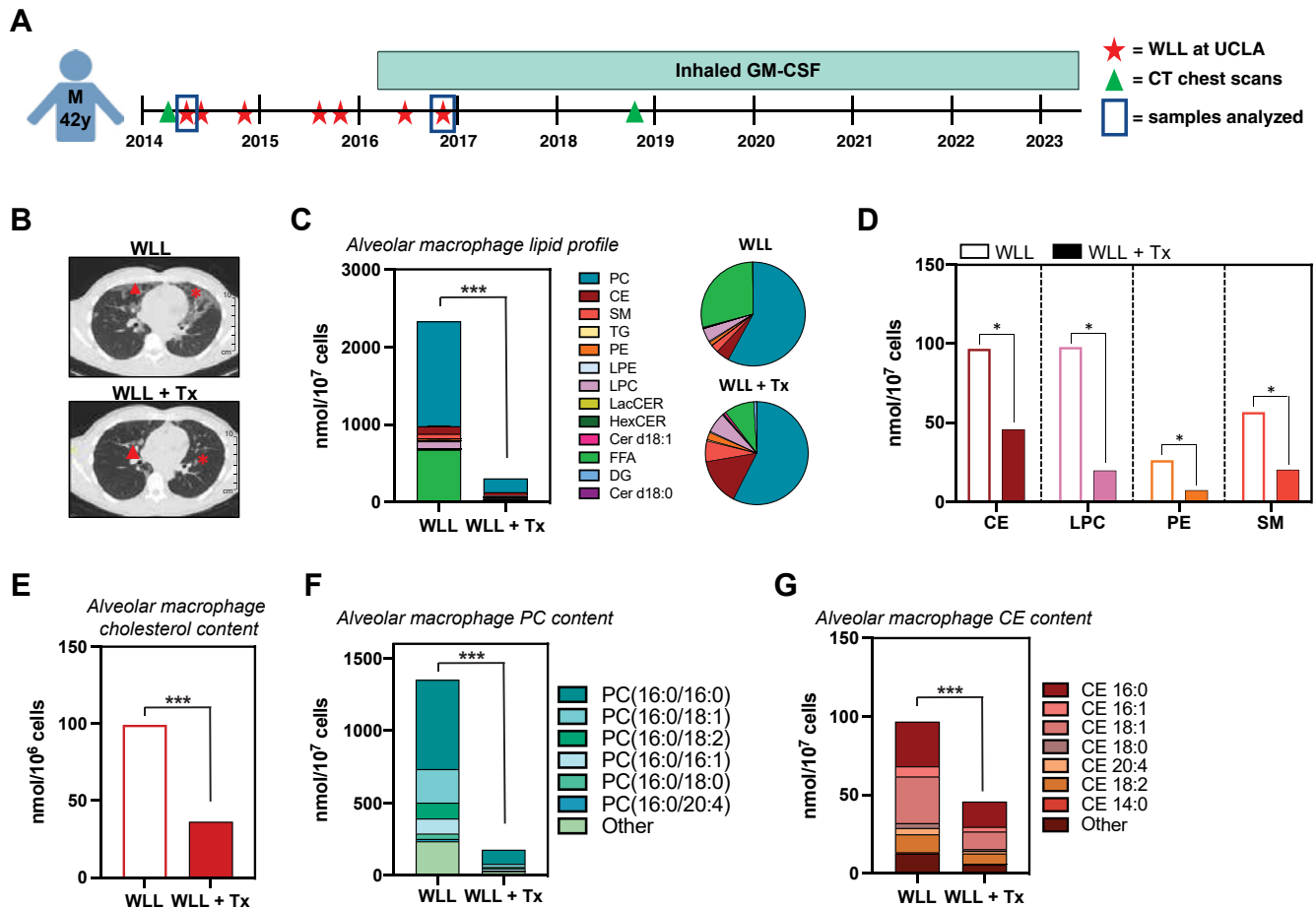
Fig. 4. Decreased alveolar macrophage lipid burden is associated with clinical improvements in PAP disease in response to therapy. (A) Clinical course of a 42-year-old patient with disease improvement after being initiated on inhaled GM-CSF. Red stars indicate whole lung lavages that were performed at UCLA. Green triangles denote when CT chest scans were taken. Blue boxes represent whole lung lavages used for analysis in (C–G). B: CT chest scans of the patient at the time of presentation to UCLA (March 2014; No Tx) and after whole lung lavage and inhaled GM-CSF therapy (November 2018; WLL+Tx). Red stars indicate ground glass opacities, and red arrowheads indicate septal thickening. C: Quantitative measurement and compositional analysis of total lipid content in alveolar macrophages of the patient before (WLL) and after initiation of inhaled GM-CSF (WLL+Tx). D: Total CE, LPC, PE, and SM content in alveolar macrophages of the patient before (WLL) and after initiation of inhaled GM-CSF (WLL+Tx). E: Total cholesterol content measured by GC/MS before (WLL) and after patient has been on inhaled GM-CSF (WLL+Tx). F–G: Absolute quantification of the most abundant PC (F) and CE (G) species in alveolar macrophages of the patient before (WLL) and after being placed on inhaled GM-CSF (WLL+Tx). Samples are run in triplicate. Data are mean ± SEM. Statistical significance determined by Mann–Whitney U-test. *$P < 0.05$, ***$P < 0.001$. Tx, treatment, which includes inhaled GM-CSF.

in 2021 after 12 months of inhaled GM-CSF therapy (supplemental Fig. S4A; blue boxes). Similar to the patient in Fig. 4 and consistent with a reduced requirement for WLL, the total lipid content and overall levels of all major lipid classes were decreased (supplemental Fig. S4C–F). Together, these data suggest that restoration of lipid homeostasis and reductions in total lipid burden correlate with clinical improvement.

In contrast, the third patient, PAP 7, had a markedly different clinical course (**Fig. 5**A). She is an otherwise healthy 34-year-old female diagnosed with aPAP in late 2017. She had two whole lung lavages before developing severe hypoxic respiratory failure requiring admission to the intensive care unit. She was initiated on inhaled GM-CSF therapy but continued to require frequent whole lung lavages (Fig. 5A). Because

of the severe nature of her disease, she received rituximab and was started on a statin, followed by pioglitazone, plasmapheresis, and additional doses of rituximab (Fig. 5A). Despite these interventions, the patient remained short of breath and hypoxic. The patient eventually underwent a bilateral lung transplant in 2021 due to declining respiratory status and worsening pulmonary fibrosis despite multiple therapies (Fig. 5A). A chest CT scan in 2020 after receiving the above therapies and prior to lung transplant (Fig. 5B; WLL+Tx) confirmed a lack of clinical improvement with evidence of ongoing diffuse ground glass opacifications (red asterisk) and septal thickening (red arrowhead) with new subpleural fibrotic changes when compared to her CT scan in 2018 (Fig. 5B; WLL).
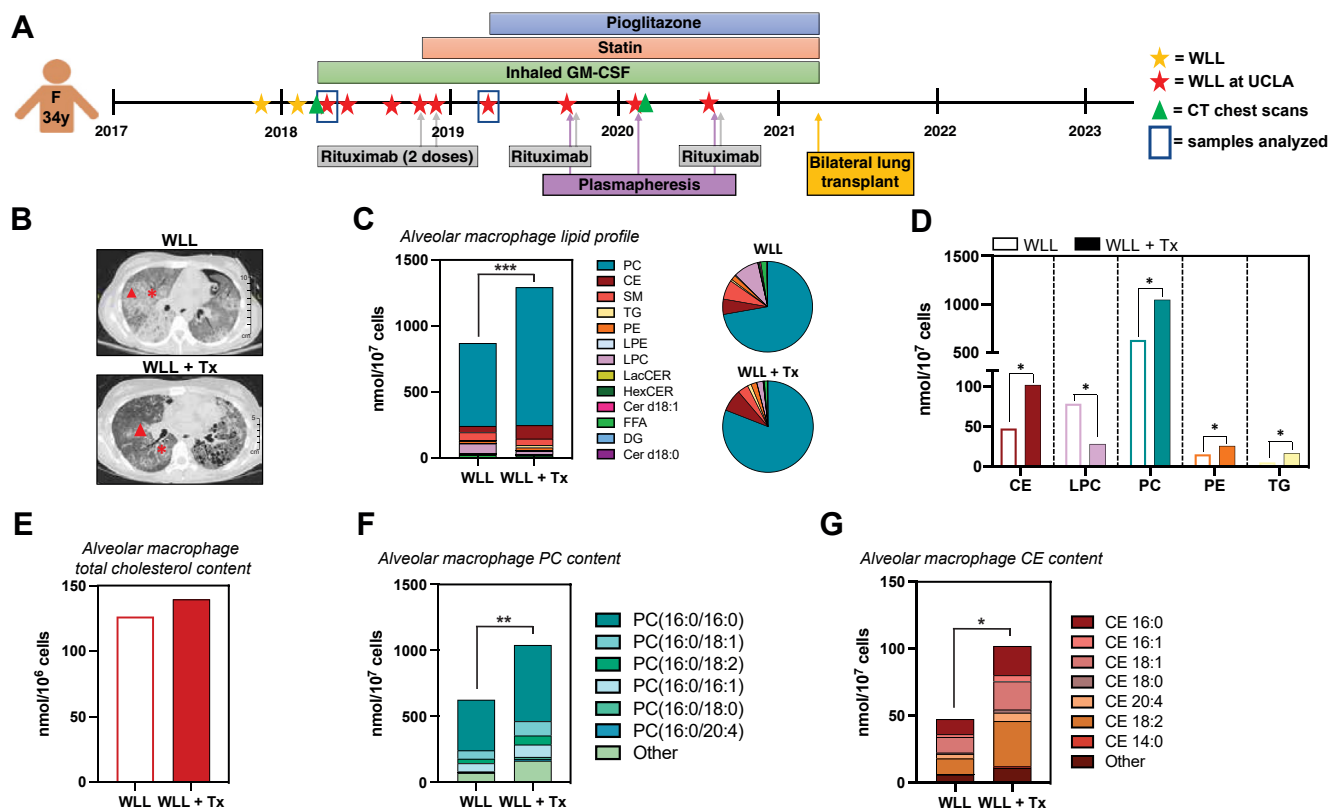
Fig. 5. Increased alveolar macrophage lipid burden is associated with worsening, unremitting disease. A: Clinical course of a 34-year-old patient with worsening PAP disease and unresolving hypoxia despite multiple therapies. Stars indicate whole lung lavages. Red stars indicate whole lung lavages that were performed at UCLA. Green triangles denote when CT chest scans were taken and shown in (B). Blue boxes represent when the whole lung lavages from the patient were used for analysis in (D–H). B: CT chest scans of the patient at the time of presentation to UCLA (April 2018; WLL) and after multiple therapies (January 2020; WLL+Tx). Red stars indicate ground glass opacities, and red arrowheads indicate septal thickening. C: Quantitative measurement and compositional analysis of total lipid content in alveolar macrophages of the patient before (WLL) and after initiation of inhaled GM-CSF (WLL+Tx). D: Total CE, LPC, PE, and SM content in alveolar macrophages of the patient before (WLL) and after initiation of inhaled GM-CSF (WLL+Tx). E: Total cholesterol content measured by GC/MS before (WLL) and after patient has been on inhaled GM-CSF (WLL+Tx). F–G: Absolute quantification of the most abundant PC (F) and CE (G) species in alveolar macrophages of the patient before (WLL) and after being placed on inhaled GM-CSF (WLL+Tx). Samples are run in triplicate. Data are mean ± SEM. Statistical significance determined by Mann–Whitney U-test. *$P < 0.05$, **$P < 0.01$, ***$P < 0.001$. Tx, treatment, which includes inhaled GM-CSF.

Alveolar macrophages were obtained when the patient was first on inhaled GM-CSF and after initiation on a statin (Fig. 5A; blue boxes). Analysis of the lipid profile of the patient's alveolar macrophages indicated that the most abundant lipid classes were PC, CE, SM, and LPC, which differed from both non-PAP patients and patient PAP 1 (Fig. 5C, D compared with Figs. 2B and 4C, respectively). Both total PC and CE levels in alveolar macrophages significantly increased as the patient's disease worsened (Fig. 5C, D), whereas total macrophage cholesterol levels were only modestly increased (Fig. 5E). The fatty acid composition of PC and CE species in the alveolar macrophages was not significantly altered as the patient's disease progressed; however, the total amount of both PC and CE was increased 2-fold in just over a year (Fig. 5F, G). We also noted similar trends in another patient PAP 8, who demonstrated little to no clinical improvement despite being treated with WLL and inhaled GM-CSF. She ultimately developed pulmonary fibrosis and underwent

a bilateral lung transplant in 2020 (supplemental Fig. S5). Unfortunately, she later died due to transplant complications. Alveolar macrophages were obtained after initiation of inhaled GM-CSF in 2019 and prior to lung transplant (supplemental Fig. S5; blue boxes). As the patient's disease worsened, CE levels significantly increased, while total PC and cholesterol levels decreased (supplemental Fig. S5C–F). Total alveolar macrophage lipid burden did not change (supplemental Fig. S5C). Taken together with our observations above (Figs. 4 and 5 and supplemental Fig. S4), these data suggest that changes in overall alveolar macrophage lipid burden are most reflective of a patient's clinical progress.

DISCUSSION

PAP is a rare, life-threatening syndrome of lipid accumulation in the alveolar space and particularly within alveolar macrophages (4). Alveolar macrophages

are crucial immune cells responsible for clearing debris and foreign substances, as well as maintaining surfactant homeostasis in the lungs, and are the main cellular target of the downstream effects of autoantibodies to GM-CSF. Despite the significance of alveolar macrophages in PAP, lipid profiles of isolated alveolar macrophages from PAP patients have not been previously reported. To address this knowledge gap, we conducted the first comprehensive study to define the lipidome of human alveolar macrophages in PAP. We show that in comparison to alveolar macrophages recovered from non-PAP patients, PAP-afflicted alveolar macrophages exhibited increased levels of numerous lipids, expanding upon the previously reported elevation in PC (7–9, 11–13, 15, 19, 25, 26). These findings indicate that there are broader changes in lipid metabolism within PAP alveolar macrophages than previously observed through more qualitative analyses. Importantly, our study highlights the significant heterogeneity of PAP as the lipid composition within alveolar macrophages varies considerably among individual patients. This variability underscores the diverse nature of the disease and points to potential differences in disease severity and progression.

Previously, lipid profiling studies in PAP have focused on analyzing lipids within the BALF in the alveolar space (19). By directly studying alveolar macrophage lipidomes, we aimed to bridge the knowledge gap in understanding the lipid abnormalities in cells known to drive PAP. A previous study reported an overall increase of total lipid concentration within the BALF recovered from the alveolar airspace with free cholesterol being increased the most (60-fold), followed by CE and PC (19). It is worth noting that comparing our findings with these previous studies posed significant challenges due to differences in sample preparation and methodology. In their reported sample preparation, WLL fluid from healthy individuals was centrifuged to remove cellular content, and the remaining cell-free lavage fluid was analyzed by direct flow injection electrospray ionization tandem mass spectrometry. However, in the case of PAP patients, unprocessed lavage fluid including cellular components was utilized for analysis. Because lavage fluid is a complex mixture of surfactant, alveolar macrophages, proteinaceous material, and in some cases other cell types, the inclusion and/or exclusion of these components can significantly affect lipidomic data and interpretation of results. Hence, a direct comparison between our findings and those reported by other researchers is not feasible.

There are currently no quantitative measures of disease burden for PAP patients. In addition, there are no studies on macrophage lipid profiles and disease progression or regression. We noted that the absolute abundance of lipids correlated with disease severity in patients with improving or persistent, worsening clinical disease. Additional studies will be required to determine whether the alveolar macrophage lipidome or a specific combination of lipids could be used as a biomarker to determine severity of disease or predict response to therapy in PAP.

Alveolar macrophages are the main cell type affected by loss of normal GM-CSF signaling in PAP (4). Our previous study demonstrated that treatment of a subset of PAP patients with statins led to a remarkable improvement in their clinical symptoms, likely by reducing alveolar macrophage cholesterol content [18]. Whether statins affect the macrophage CE species in the treatment-responsive patients is currently unknown. Additionally, not all patients respond to statin therapy, suggesting that there is a need for further studies on the lipidome of alveolar macrophages and molecular targets. Furthermore, there is also a subset of PAP patients whose disease is stable, and these patients do not require WLL therapy. Detailed study of the alveolar macrophage lipidome of these patients will be extremely interesting and could provide further valuable insights into the disease mechanisms.

In conclusion, expanding our understanding of the lipidome in alveolar macrophages from a larger cohort of PAP patients, including those undergoing different therapies, is crucial for gaining further insights into disease pathogenesis, discovering robust biomarkers for disease severity and prediction of treatment response prediction, as well as identifying potential therapeutic targets. By elucidating the complex lipid abnormalities and heterogeneity within alveolar macrophages, we can pave the way for more personalized and effective approaches to managing and treating PAP disease.

Data availability

The data supporting this study are available in the article, the supplemental data, or from the corresponding author upon request.

T. funding acquisition; T. Q. de A. V., T. W., and E. J. T. supervision; E. J. T. project administration.

Author ORCIDs
Elinor Lee https://orcid.org/0000-0003-3008-8325
Kevin J. Williams https://orcid.org/0000-0001-8091-7924
Cormac McCarthy https://orcid.org/0000-0003-2896-5210
James P. Bridges https://orcid.org/0000-0002-4815-117X
Elizabeth F. Redente https://orcid.org/0000-0002-8075-4325
Thomas Q. de Aguiar Vallim https://orcid.org/0000-0001-7642-5046
Elizabeth J. Tarling https://orcid.org/0000-0002-0599-0432

Conflict of interest
The authors declare that they have no conflicts of interest with the contents of this article.

Abbreviations
aPAP, autoimmune PAP; BAL, bronchoalveolar; BALF, bronchoalveolar lavage fluid; CE, cholesterol esters; Cer d18:1, ceramides; Cer d18:0, dihydroceramides; DG, diacylglycerols; FFA, free fatty acids; GC-MS, gas chromatography/mass spectrometry; GM-CSF, granulocyte macrophage colony stimulating factor; HexCER, hexosylceramides; LacCER, lactosylceramides; LPC, lysophosphatidylcholines; LPE, lysophosphatidylethanolamines; PAP, pulmonary alveolar proteinosis; PC, phosphatidylcholines; PE, phosphatidylethanolamines; SM, sphingomyelins; TG, triacylglycerols; Tx, treatment; WLL, whole lung lavage.

REFERENCES

1. Trapnell, B. C., Whitsett, J. A., and Nakata, K. (2003) Pulmonary alveolar proteinosis. *N. Engl. J. Med.* **349**, 2527–2539
2. Trapnell, B. C., Nakata, K., Bonella, F., Campo, I., Griese, M., Hamilton, J., *et al* (2019) Pulmonary alveolar proteinosis. *Nat. Rev. Dis. Primers.* **5**, 16
3. McCarthy, C., Avetisyan, R., Carey, B. C., Chalk, C., and Trapnell, B. C. (2018) Prevalence and healthcare burden of pulmonary alveolar proteinosis. *Orphanet J. Rare Dis.* **13**, 129
4. McCarthy, C., Carey, B. C., and Trapnell, B. C. (2022) Autoimmune pulmonary alveolar proteinosis. *Am. J. Respir. Crit. Care Med.* **205**, 1016–1035
5. Hamilton, J. A. (2008) Colony-stimulating factors in inflammation and autoimmunity. *Nat. Rev. Immunol.* **8**, 533–544
6. Guilliams, M., De Kleer, I., Henri, S., Post, S., Vanhoutte, L., De Prijck, S., *et al* (2013) Alveolar macrophages develop from fetal monocytes that differentiate into long-lived cells in the first week of life via GM-CSF. *J. Exp. Med.* **210**, 1977–1992
7. Dranoff, G., Crawford, A. D., Sadelain, M., Ream, B., Rashid, A., Bronson, R. T., *et al* (1994) Involvement of granulocyte-macrophage colony-stimulating factor in pulmonary homeostasis. *Science.* **264**, 713–716
8. Shima, K., Arumugam, P., Sallese, A., Horio, Y., Ma, Y., Trapnell, C., *et al* (2022) A murine model of hereditary pulmonary alveolar proteinosis caused by homozygous Csf2ra gene disruption. *Am. J. Physiol. Lung Cell Mol. Physiol.* **322**, L438–L448
9. Robb, L., Drinkwater, C. C., Metcalf, D., Li, R., Kontgen, F., Nicola, N. A., *et al* (1995) Hematopoietic and lung abnormalities in mice with a null mutation of the common beta subunit of the receptors for granulocyte-macrophage colony-stimulating factor and interleukins 3 and 5. *Proc. Natl. Acad. Sci. U. S. A.* **92**, 9565–9569
10. Ohkouchi, S., Akasaka, K., Ichiwata, T., Hisata, S., Iijima, H., Takada, T., *et al* (2017) Sequential granulocyte-macrophage colony-stimulating factor inhalation after whole-lung lavage for pulmonary alveolar proteinosis. A report of five intractable cases. *Ann. Am. Thorac. Soc.* **14**, 1298–1304
11. McCarthy, C., Lee, E., Bridges, J. P., Sallese, A., Suzuki, T., Woods, J. C., *et al* (2018) Statin as a novel pharmacotherapy of pulmonary alveolar proteinosis. *Nat. Commun.* **9**, 3127
12. Sallese, A., Suzuki, T., McCarthy, C., Bridges, J., Filuta, A., Arumugam, P., *et al* (2017) Targeting cholesterol homeostasis in lung diseases. *Sci. Rep.* **7**, 10211–10214
13. Thomassen, M. J., Barna, B. P., Malur, A. G., Bonfield, T. L., Farver, C. F., Malur, A., *et al* (2007) ABCG1 is deficient in alveolar macrophages of GM-CSF knockout mice and patients with pulmonary alveolar proteinosis. *J. Lipid Res.* **48**, 2762–2768
14. Baldan, A., Tarr, P., Vales, C. S., Frank, J., Shimotake, T. K., Hawgood, S., *et al* (2006) Deletion of transmembrane transporter ABCG1 results in progressive pulmonary lipidosis. *J. Biol. Chem.* **281**, 29401–29410
15. Bonfield, T. L., Farver, C. F., Barna, B. P., Malur, A., Abraham, S., Raychaudhuri, B., *et al* (2003) Peroxisome proliferator-activated receptor-gamma is deficient in alveolar macrophages from patients with alveolar proteinosis. *Am. J. Respir. Cell Mol. Biol.* **29**, 677–682
16. Kennedy, M. A., Barrera, G. C., Nakamura, K., Baldan, A., Tarr, P., Fishbein, M. C., *et al* (2005) ABCG1 has a critical role in mediating cholesterol efflux to HDL and preventing cellular lipid accumulation. *Cell Metab.* **1**, 121–131
17. de Aguiar Vallim, T. Q., Lee, E., Merriott, D. J., Goulbourne, C. N., Cheng, J., Cheng, A., *et al* (2017) ABCG1 regulates pulmonary surfactant metabolism in mice and men. *J. Lipid Res.* **58**, 941–954
18. Ferretti, A., Fortwendel, J. R., Gebb, S. A., and Barrington, R. A. (2016) Autoantibody-mediated pulmonary alveolar proteinosis in Rasgrp1-deficient mice. *J. Immunol.* **197**, 470–479
19. Griese, M., Bonella, F., Costabel, U., de Blic, J., Tran, N. B., and Liebisch, G. (2019) Quantitative lipidomics in pulmonary alveolar proteinosis. *Am. J. Respir. Crit. Care Med.* **200**, 881–887
20. Baldan, A., Gonen, A., Choung, C., Que, X., Marquart, T. J., Hernandez, I., *et al* (2014) ABCG1 is required for pulmonary B-1 B cell and natural antibody homeostasis. *J. Immunol.* **193**, 5637–5648
21. Bligh, E. G., and Dyer, W. J. (1959) A rapid method of total lipid extraction and purification. *Can J. Biochem. Physiol.* **37**, 911–917
22. Hsieh, W., Williams, K. J., Su, B., and Bensinger, S. J. (2020) Profiling of mouse macrophage lipidome using direct infusion shotgun mass spectrometry. *STAR Protoc.* **2**, 100235
23. Su, B., Bettcher, L. F., Hsieh, W-Y., Hornburg, D., Pearson, M. J., Blomberg, N., *et al* (2021) A DMS shotgun lipidomics workflow application to facilitate high-throughput, comprehensive lipidomics. *J. Am. Soc. Mass Spectrom.* **32**, 2655–2663
24. Veldhuizen, R., Nag, K., Orgeig, S., and Possmayer, F. (1998) The role of lipids in pulmonary surfactant. *Biochim. Biophys. Acta.* **1408**, 90–108
25. Ikegami, M.,U. T., Hull, W., Whitsett, J. A., Mulligan, R. C., Dranoff, G., and Jobe, A. H. (1996) Surfactant metabolism in transgenic mice after granulocyte macrophage-colony stimulating factor ablation. *Am. J. Physiol.* **270**, L650–L658
26. Baker, A. D., Malur, A., Barna, B. P., Ghosh, S., Kavuru, M. S., Malur, A., *et al* (2010) Targeted PPAR{gamma} deficiency in alveolar macrophages disrupts surfactant catabolism. *J. lipid Res.* **51**, 1325–1331